SUPPORTING INFORMATION

Supporting Figures

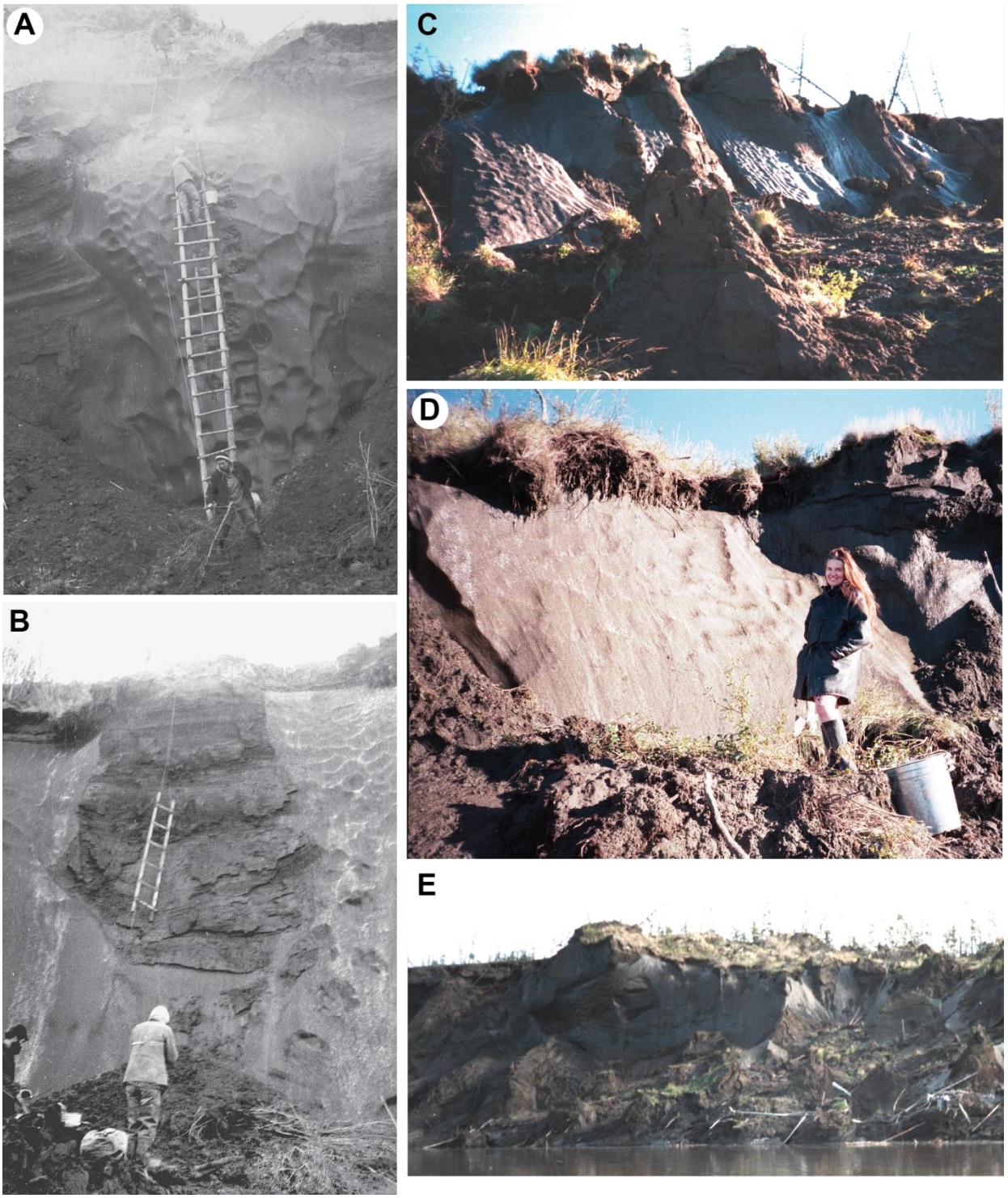

Figure S1 Ice wedges at Duvanny Yar. (A) Lower part of large syngenetic wedge, yedoma section II, September 1985. (B) Uppermost part of large syngenetic wedge, yedoma section III, September 1985. (C) Uppermost part of thin syngenetic wedge, yedoma section I, August 1999. (D) Uppermost part of yedoma section I, August 1999. (E) General view, August 1999. Photographs are by Yurij Vasil'chuk.

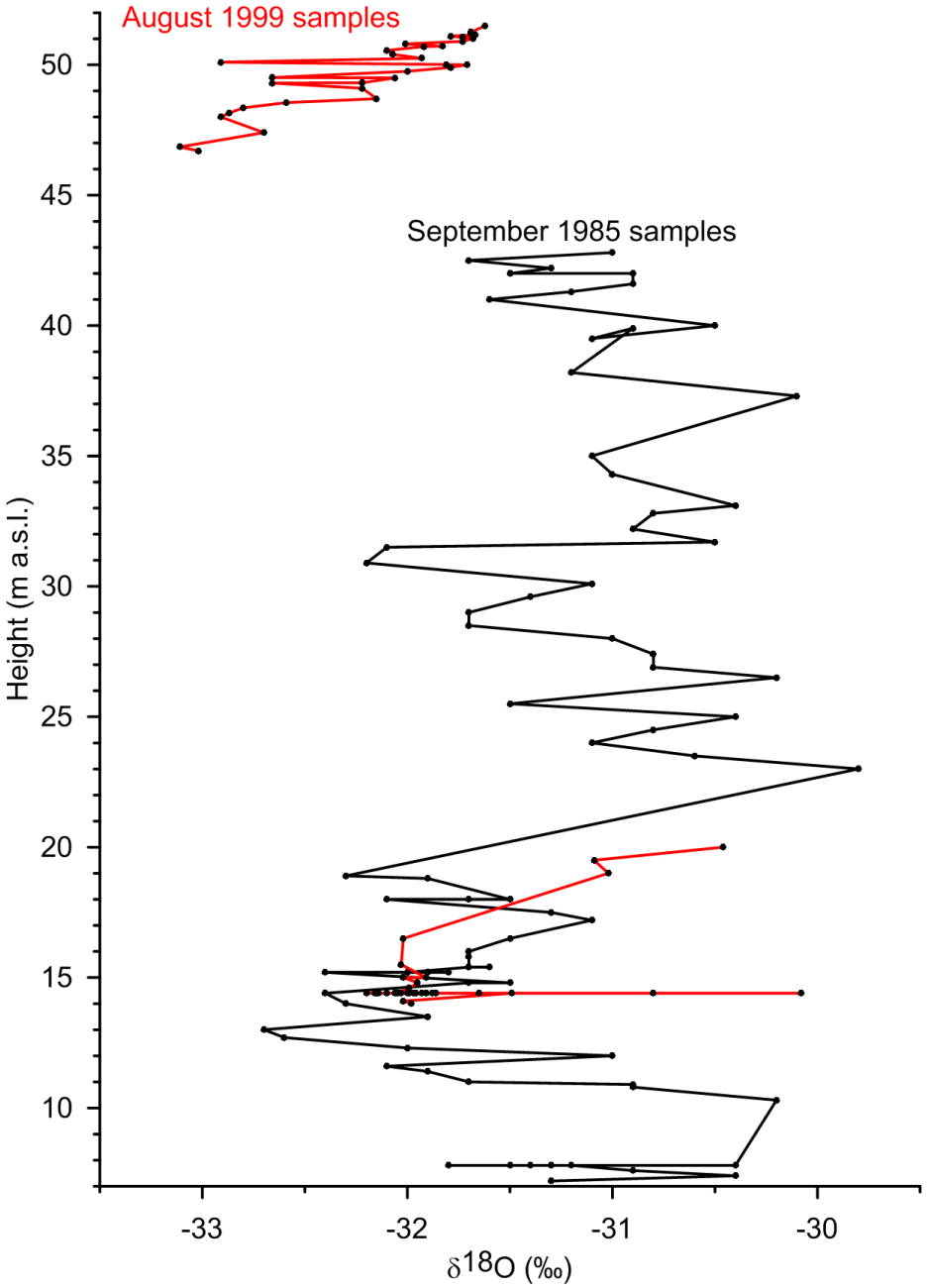

Figure S2 $\delta^{18}O$ plots of syngenetic wedge ice at Duvanny Yar. Sampling by Y. K. Vasil'chuk and A. C. Vasil'chuk.

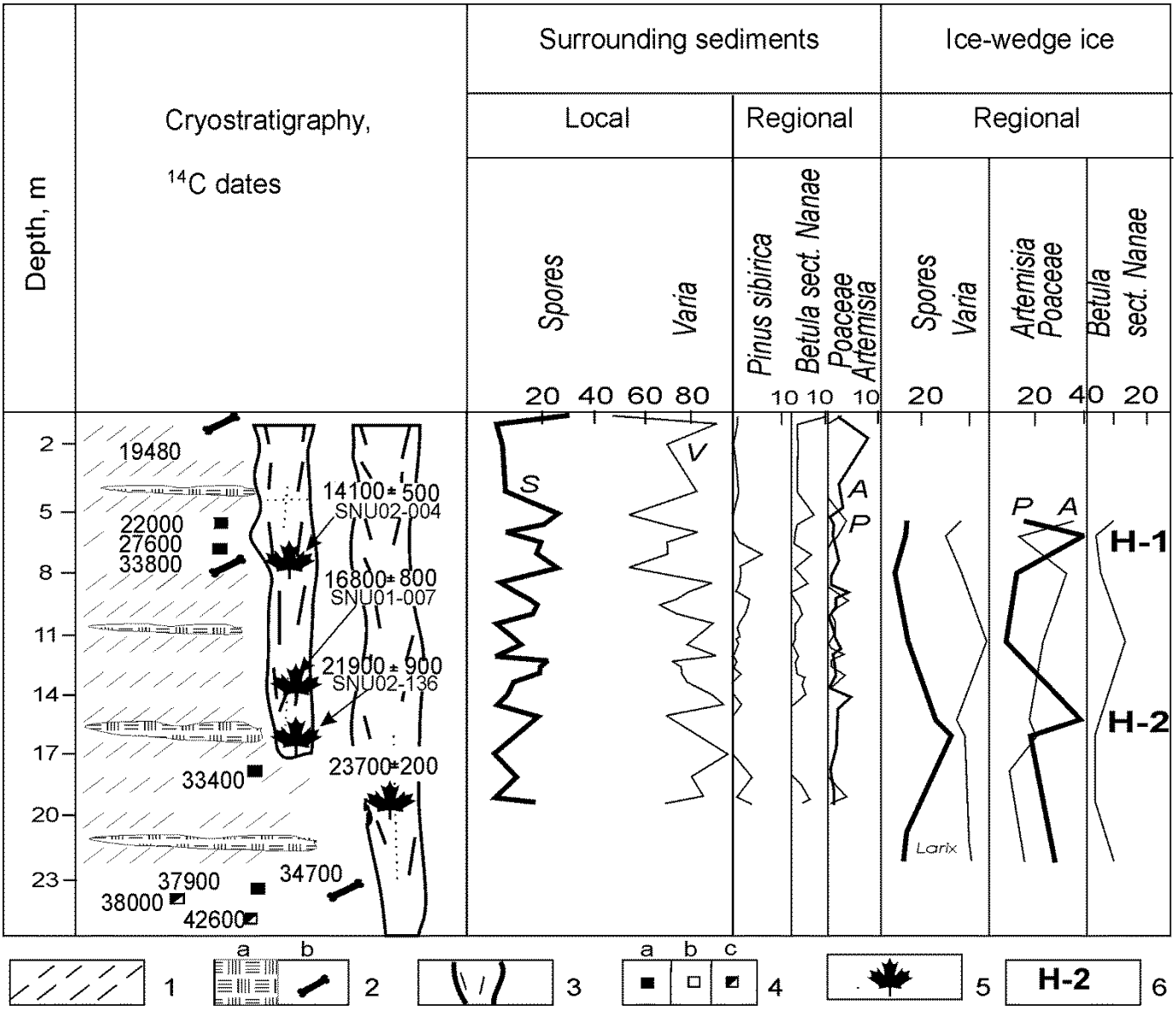

Figure S3 Pollen and spores in wedge ice and surrounding yedoma sediments at Duvanny Yar. 1 – sandy loam; 2 – plant remains and peat (a), bones (b); 3 – large syngenetic ice wedges; 4 – sampling point for ^{14}C dating: a – rootlets, b – branches, c – dispersed organic plant material: 5 – sampling point from ice-wedge ice: for AMS ^{14}C dating of pollen concentrate; 6 – a cold phase of Heinrich events on pollen curve. Latin letters near to pollen curves indicate first letter of the name of the appropriate plant. (after Y. K. Vasil'chuk and A. C. Vasil'chuk, 2008)

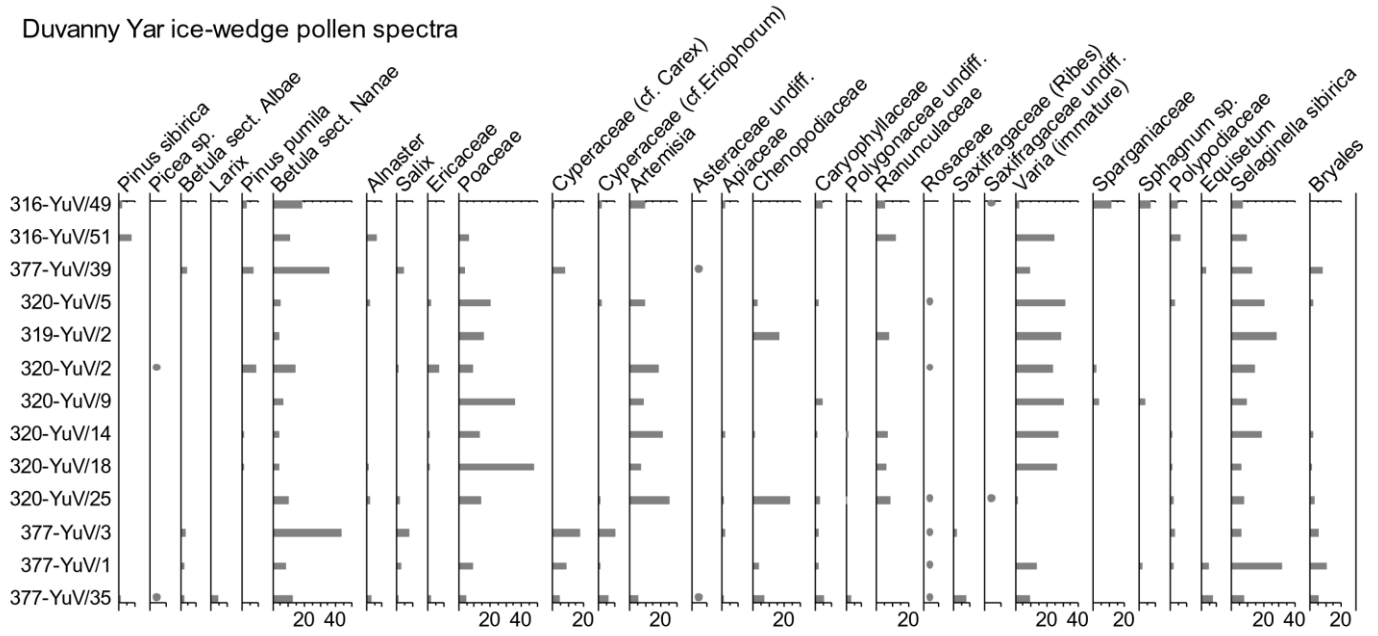

Figure S4 Pollen spectra from wedge ice at Duvanny Yar. Samples collected in 1985 and 1999 sampling programmes by A. C. Vasil'chuk and Y. K. Vasil'chuk.

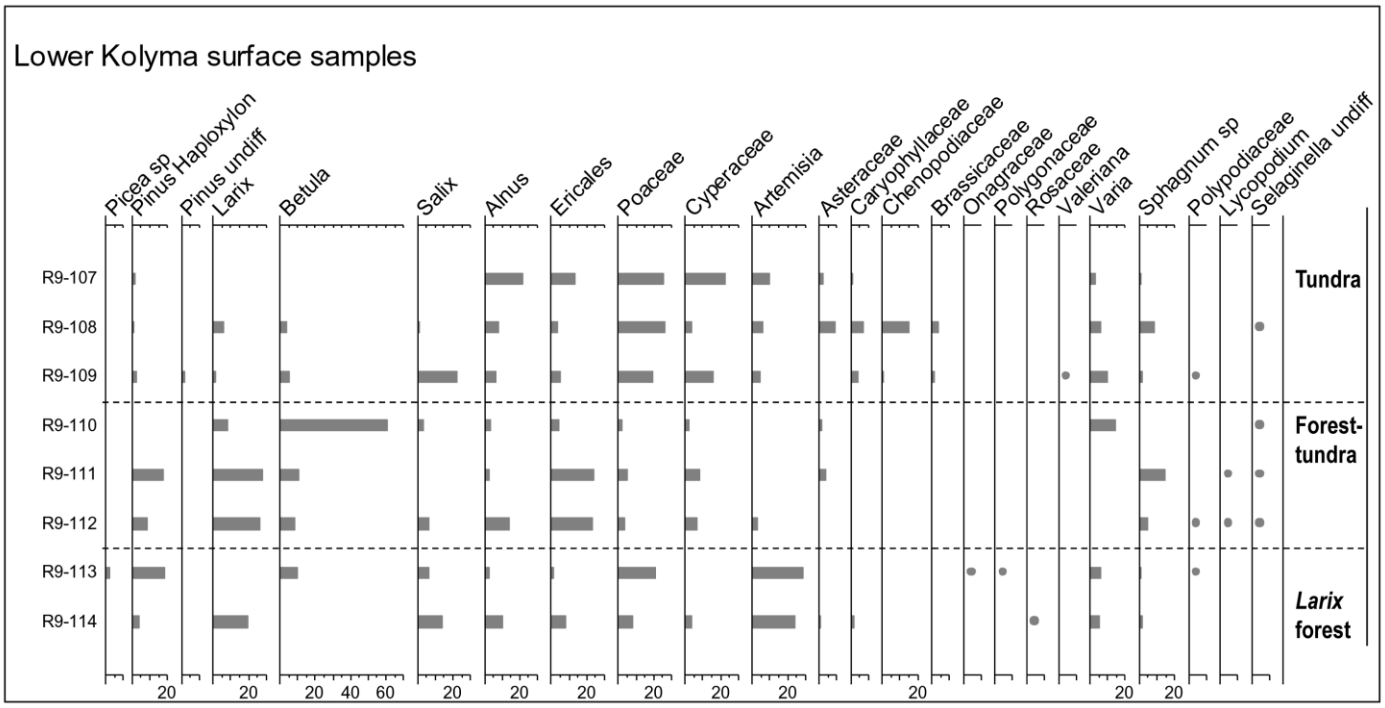

Figure S5 Modern surface pollen spectra in the lower Kolyma region. Samples collected by Andrei Sher.

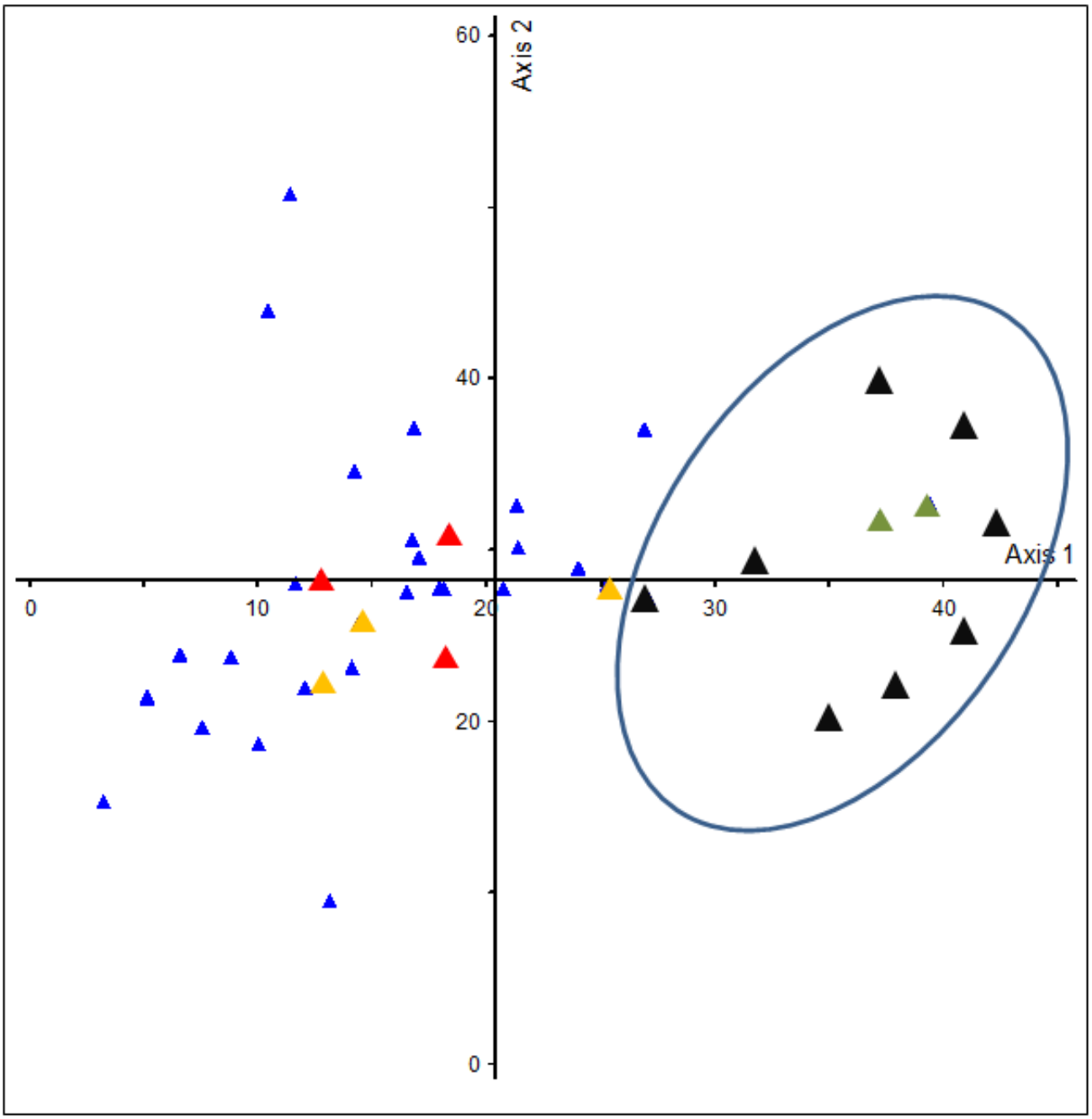

Figure S6 Bi-plot of fossil and modern pollen sample scores from Duvanny Yar and the lower Kolmya region on the first two axes of a detrended correspondence analysis (DCA). The oval encloses all surface samples (black triangles) indicated in Figure S5 and the two Holocene samples (green triangles) from pollen zone A in near-surface silt of unit 5 at Duvanny Yar (Figure 26). Red triangles are fossil samples from pollen zone B (attributed to the Last Glacial Maximum [LGM]) of yedoma silt in unit 4, and blue triangles are fossil samples from pollen zones C and D in yedoma silt of unit 4 that are older then the LGM and younger than the last interglacial (LIG). Gold triangles are from fossil samples in massive silt of unit 1 (attributed to Marine Isotope Stage [MIS] 6; Figure 25).

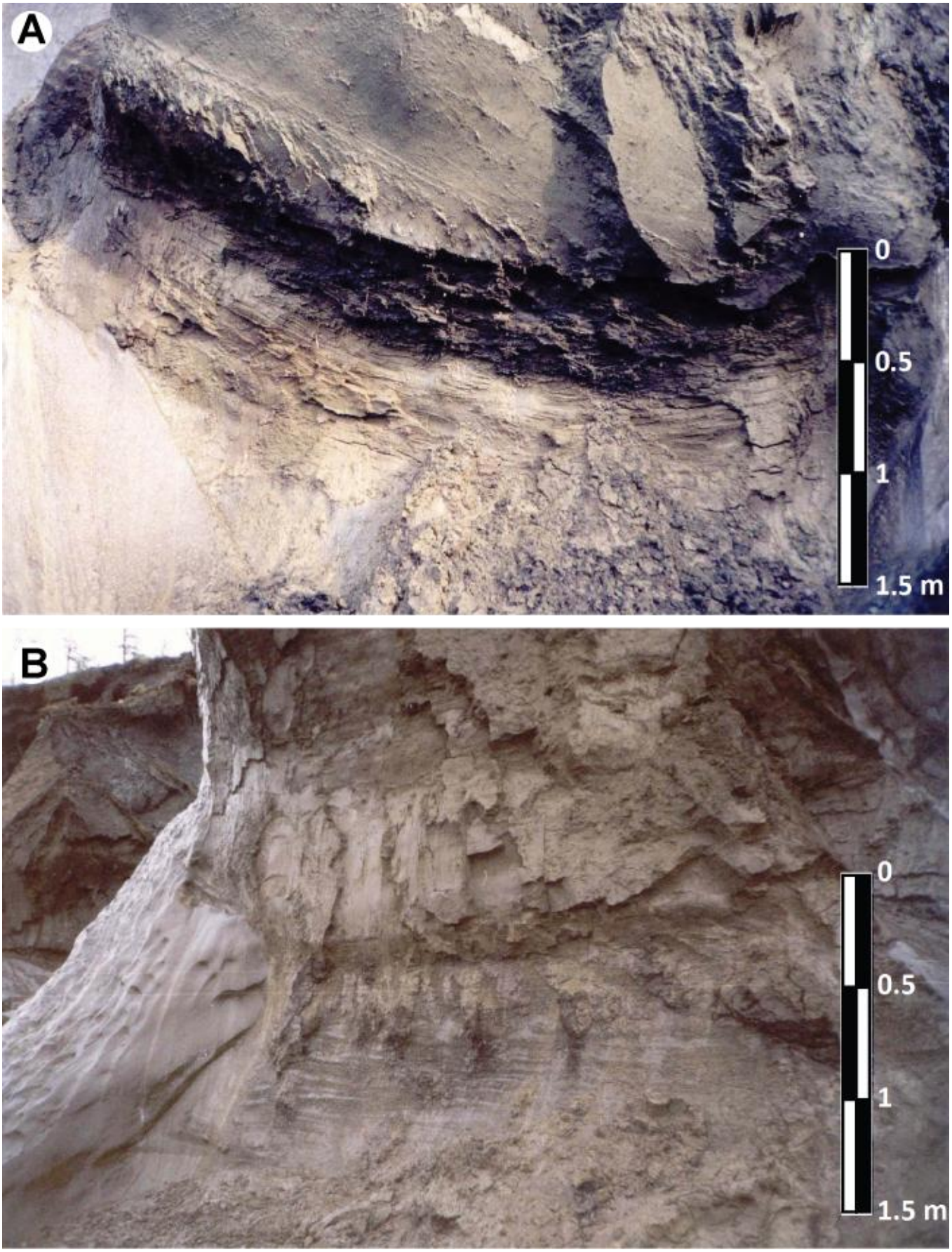

Figure S7 Profiles of palaeosols 3 and 4, from 20 and 27 m arl, respectively, in yedoma remnant 6E, Duvanny Yar. (A) Palaeosol 3: 38,000–35,000 ^{14}C BP (Late Karginskian first-stage buried soil 2), and (B) Palaeosol 4: 33,000–31,000 ^{14}C BP (Late Karginskian second-stage buried soil 3). arl = Above river level. Photographs are by Stanislav Gubin (2002).

Figure S8 Buried palaeosol profiles in the yedoma exposure of Stanchikovsky Yar (Malyy Anyuy River). Photograph is by Oksana Zanina (2002) and Gubin and Lupachev (2012).

Supporting Tables

Table S1 ^{14}C ages previously obtained from organic material in the yedoma at Duvanny Yar (unit 4 of the present study).

Study	Radiocarbon age (yr BP)	Laboratory Number	Height above sea level (m)	Organic Material
T. N. Kaplina, sampling 1972 (published in Kaplina, 1986)	17850 ± 110	MAG-592	about 42	Dispersed amorphous organic plant material (DAOPM)
	31100 ± 400	GIN-2280	20	DAOPM
	33800±1400	GIN-2279	12	DAOPM
	38000 ± 1400	GIN-2277	12	DAOPM
	37600 ± 1100	MSU-468	about 11	Peat (possibly autochthonous)
	38000 ± 2000	GIN-1688	9.5	DAOPM
	36900 ± 500	MSU -469	8.5	Peat (possibly autochthonous)
	>45000	MSU -573	6	Wood
S. V. Tomirdiaro and B. I. Chyornen'kiy, sampling 1985 (published in Tomirdiaro and Chyornen'kiy, 1987)	24070 ± 410	SOAN-2302	about 42	Detrital peat
	26060 ± 650	Lu-1675	about 42	Detrital peat
	34025 ± 550	SOAN -2303	about 40	Detrital peat
	34400 ± 1010	Lu-1674	about 40	Detrital peat
	42840 ± 2400	Lu-1676	about 38	Detrital peat
	48410 ± 3145	SOAN -2304	about 38	Detrital peat
	>50000	SOAN -2305	about 14	Wood
	>53370	Lu-1678	about 14	Wood
Y. K. Vasil'chuk and L. Sulerzhitsky, sampling 1985 (published in Y. K. Vasil'chuk, 1992)	19480 ± 100	GIN-3868	45.5	Horse bone
	22000 ± 800	GIN-4017	41.0	Rootlets (possibly *in situ*)
	27600 ± 1000	GIN-4016	39.0	DAOPM
	33800 ± 500	GIN-3861	39.0	Bone
	33400 ± 500	GIN-4018	30.0	DAOPM
	37900 ± 1000	GIN-4015	25.0	Allochthonous rootlets
	34700 ± 400	GIN-4434	25.0	Bone
	45400 ± 1200	GIN-3860	24.0	Bone
	35100 ± 100	GIN-3865	21.0	Black Soil
	38000 ± 500	GIN-3864	20.5	Allochthonous sprigs (small branches)
	42600 ± 1200	GIN-3862	19.0	Allochthonous sprigs (small branches)
	>50000	GIN-3866	19.0	Horse bone
	28600 ± 300	GIN-3867	15.0	Mammoth bone
	44200 ± 1100	GIN-4003	14.0	DAOPM
	33500 ± 1100	GIN-4006	13.0	Rootlets (possibly *in situ*)
	44600 ± 1200	GIN-4000	10.0	Allochthonous rootlets
	35500 ± 700	GIN-3999	9.5	Allochthonous rootlets
	30100 ± 800	GIN-3998	9.0	Rootlets (possibly *in situ*)
	>53000	GIN-3857	9.0	Mammoth tusk
	45200 ± 1100	GIN-3852	8.0	Allochthonous sprigs (small branches)
	36800 ± 800	GIN-3997	8.0	Rootlets (possibly *in situ*)
	35400 ± 900	GIN-3996	7.5	Rootlets (possibly *in situ*)
S. V. Gubin, 1999 (published in Gubin, 1999)	13080 ± 140	EP-941555	about 51	Soil
	28100 ±700	GIN-7697	about 36	Soil
	31100 ± 900	GIN-8016	about 26	Soil
	42400 ± 1100	GIN-9596	about 15	Soil
	43800 ± 1700	GIN-9595	about 14	Soil
F. Romanenko (unpublished date)	20000 ± 1300	GIN-7696	Beach	Deer bone (assumed to derive from yedoma in unit 4)

Table S2 The youngest ^{14}C ages obtained in each horizon of yedoma at Duvanny Yar.

Radiocarbon age (yr BP)	Laboratory Number	Height above sea level (m)	Organic Material
13080±140	EP-941555	about 51	Soil
17850 ± 110	MAG-592	about 42	Dispersed amorphous organic plant material (DAOPM)
28600 ± 300	GIN-3867	18.0	Mammoth bone
35400 ± 900	GIN-3996	7.5	DAOPM

From Y. K. Vasil'chuk (2006)

Table S3 Conventional ^{14}C age from a bulk sample of Duvanny Yar yedoma (from a sequence in Table S1) and AMS ^{14}C ages for its different organic fractions.

Field Number	Height above sea level (m)	^{14}C age of bulk sample	Organic fractions	AMS ^{14}C ages (yr BP) & Laboratory Number	$\delta^{13}C$ value (‰)
316-YuV/9	14.0	44200 ± 1100 (GIN-4003) – hot alkaline extract	Seed fragments	45700 ± 1200 (SNU01-077)	–32.4
			Thin white twigs without crust	40500 ± 500 (SNU01-078)	–25.6
			Herb remains and detritus	39000 ± 1300 (SNU01-079)	–

From Y. K. Vasil'chuk (2006)

Table S4 AMS ^{14}C ages of organic material from wedge ice at Duvanny Yar.

Field Number	Height above sea level (m) / depth below ground surface (m)	Organic fractions	AMS ^{14}C ages (yr BP)	Laboratory Number	$\delta^{13}C$ values (‰)
The lower part of the downstream section, sampling 1985					
316-YuV/53	18.9 (29.1)	Organic microinclusions	31900 ± 2800	SNU02-135	–27.5
316-YuV/50	10.6 (37.4)	Organic microinclusions	25200 ± 400	SNU02-134	–23.1
316-YuV/47	9.7 (38.3)	Organic microinclusions	31200 ± 600	SNU01-004	–27.3
316-YuV/25	7.8 (40.2)	Organic microinclusions	25900 ± 300	SNU02-006	–32.0
316-YuV/23	7.8 (40.2)	Organic microinclusions	36500 ± 800	SNU02-133	–23.2
The middle part of the middlestream section, sampling 1985					
320-YuV/15	41.0 (7.0)	Organic microinclusions	14100 ± 500	SNU02-004	–30.3
320-YuV/17	37.4 (11.6)	Organic microinclusions	20100 ± 1400	SNU02-137	–24.1
320-YuV/8	35.0 (13.0)	Organic microinclusions	16800 ± 800	SNU01-007	–46.7
320-YuV/3	31.7 (16.3)	Organic microinclusions	25800 ± 300	SNU01-006	–35.4
320-YuV/2	31.2 (16.8)	Organic microinclusions	21900 ± 900	SNU02-136	–37.8
319-YuV/10	26.9 (21.1)	Organic microinclusions	23700 ± 200	SNU01-005	–24.1
The upper part of the upstream section, sampling 1999					
377-YuV/1	+49.5 (5.5)	Organic microinclusions	19190 ± 170	GrA-19166	–25.99
		Alkali extract	31070 ± 1510	GrA-19202	–25.51
		Organic microinclusions	40600 ± 1200	SNU02-146	–20.2
377-YuV/2	+49.3 (5.7)	Organic microinclusions	24910 ± 300	GrA-19167	–26.15
		Alkali extract	33600 ± 430	GrA-19183	–27.01
377-YuV/3	+50.1 (4.9)	Organic microinclusions	31160 ± 300	GrA-19178	–26.06
		Alkali extract	36030 ± 540	GrA-19184	–25.87
		Organic microinclusions	34600 ± 1400	SNU02-149	–18.9
377-YuV/5	+51.5 (3.5)	Organic microinclusions	24260 ± 280	GrA-19168	–25.42
		Alkali extract	32330 ± 370	GrA-19186	–26.39
377-YuV/33	+50.0 (5.0)	Organic microinclusions	26630 ± 340	GrA-19170	–25.51
		Alkali extract	31030 ± 310	GrA-19187	–26.08
377-YuV/35	+47.4 (7.6)	Organic microinclusions	28910 ± 270	GrA-19181	–25.41
		Alkali extract	32330 ± 1720	GrA-19210	–26.70
		Pollen	47100 ± 3000	SNU02-126	–
377-YuV/39	+14.0/ 41.0	Pollen	40600 ± 800	SNU02-148	–

From Y. K. Vasil'chuk *et al.* (1988, 2001a, 2004) and Y. K. Vasil'chuk (2006)

Table S5 $\delta^{18}O$ values from wedge ice in 1985 sampling programme[a] by Y. K. Vasil'chuk at Duvanny Yar.

Field number	Height asl (m) / Depth bgs (m)	$\delta^{18}O$ [‰]	Field number	Height asl (m) / Depth bgs (m)	$\delta^{18}O$ [‰]	Field number	Height asl (m) / Depth bgs (m)	$\delta^{18}O$ [‰]
320-YuV/27	42.8/5.2	–31.0	319-YuV/8	28.0/20.0	–31.0	316-YuV/98	15.2/32.8	–31.9
320-YuV/26	42.5/5.5	–31.7	319-YuV/9	27.4/20.6	–30.8	316- YuV/92	15.2/32.8	–32.4
320-YuV/25	42.2/5.8	–31.3	319-YuV/10	26.9/21.1	–30.8	316- YuV/91	14.8/33.2	–31.5
320-YuV/24	42.0/6.0	–31.5	319-YuV/11	26.5/21.5	–30.2	316-YuV/90	14.8/33.2	–31.7
320-YuV/23	42.0/6.0	–31.5	319-YuV/12	26.0/22.0	–30.9	316-YuV/89	14.4/33.6	–32.4
320-YuV/22	42.0/6.0	–31.5	319-YuV/13	25.5/22.5	–31.5	316-YuV/88	14.0/34.0	–32.3
320-YuV/20	42.0/6.0	–30.9	319-YuV/14	25.0/23.0	–30.4	316-YuV/87	13.5/34.5	–31.9
320-YuV/18	41.6/6.4	–30.9	319-YuV/15	24.5/23.5	–30.8	316-YuV/86	13.0/35.0	–32.7
320-YuV/17	41.3/6.7	–31.2	319-YuV/16	24.0/24.0	–31.1	316-YuV/85	12.7/35.3	–32.6
320-YuV/15	41.0/7.0	–31.6	319-YuV/17	23.5/24.5	–30.6	316-YuV/84	12.3/35.7	–32.0
320-YuV/14	40.0/8.0	–30.5	319-YuV/18	23.0/25.0	–29.8	316-YuV/83	12.0/36.0	–31.0
320-YuV/13	39.5/8.5	–31.1	316-YuV/53	18.9/29.1	–32.3	316-YuV/82	11.6/36.4	–32.1
320-YuV/12	39.9/9.0	–30.9	316-YuV/54	18.8/29.2	–31.9	316-YuV/81	11.4/36.6	–31.9
320-YuV/11	38.2/9.8	–31.2	316-YuV/55	18.0/30.0	–31.5	316-YuV/80	11.0/37.0	–31.7
320-YuV/10	37.3/10.7	–30.1	316-YuV/56	18.0/30.0	–31.7	316-YuV/52	10.9/37.1	–30.9
320-YuV/8	35.0/13.0	–31.1	316- YuV/57	18.0/30.0	–32.1	316-YuV/51	10.8/37.2	–30.9
320-YuV/7	34.3/13.7	–31.0	316- YuV/58	17.5/30.5	–31.3	316-YuV/49	10.3/37.7	–30.2
320-YuV/6	33.1/14.9	–30.4	316-YuV/59	17.2/30.8	–31.1	316-YuV/25	7.8/40.2	–30.4
320-YuV/5	32.8/15.2	–30.8	316-YuV/102	16.5/31.5	–31.5	316-YuV/24	7.8/40.2	–31.3
320-YuV/4	32.2/15.8	–30.9	316-YuV/101	16.0/32.0	–31.7	316- YuV/23	7.8/40.2	–31.4
320-YuV/3	31.7/16.3	–30.5	316-YuV/97	15.8/32.2	–31.7	316- YuV/20	7.8/40.2	–31.5
319-YuV/2	31.5/16.5	–32.1	316-YuV/96	15.4/32.6	–31.7	316-YuV/19	7.8/40.2	–31.3
319-YuV/3	30.9/17.1	–32.2	316-YuV/95	15.4/32.6	–31.6	316-YuV/18	7.8/40.2	–31.8
319-YuV/4	30.1/17.9	–31.1	316-YuV/94	15.4/32.6	–31.7	316-YuV/17	7.8/40.2	–31.2
319-YuV/5	29.6/18.4	–31.4	316-YuV/93	15.4/32.6	–31.7	316-YuV/16	7.6/40.4	–30.9
319-YuV/6	29.0/19.0	–31.7	316-YuV/100	15.2/32.8	–32.0	316-YuV/15	7.4/40.6	–30.4
319-YuV/7	28.5/19.5	–31.7	316-YuV/99	15.2/32.8	–31.8	316-YuV/14	7.2/40.8	–31.3

[a] Top of Duvanny Yar section in 1985 at 48 m asl; bottom at 6 m asl. asl = Above sea level; bgs = below ground surface.

Table S6 $\delta^{18}O$, $\delta^{2}H$ and d_{exc} values from ice-wedge ice in 1999 sampling programme[a] by Y. K. Vasil'chuk and A. C. Vasil'chuk at Duvanny Yar.

Field number	Height asl (m) / Depth bgs (m)	$\delta^{2}H$ [‰]	$\delta^{18}O$ [‰]	d_{exc} [‰]	Field number	Height asl (m) / Depth bgs (m)	$\delta^{2}H$ [‰]	$\delta^{18}O$ [‰]	d_{exc} [‰]
377-YuV/5	51.5/3.5	–245.6	–31.62	7.4	377-YuV/49	19.5/35.5	–239.5	–31.09	9.2
377-YuV/11	51.25/3.75	–246.2	–31.69	7.3	377-YuV/50	19.0/36.0	–238.6	–31.02	9.6
377-YuV/10	51.2/3.8	–246.4	–31.69	7.1	377-YuV/75	16.5/38.5	–248.8	–32.02	7.4
377-YuV/9	51.15/3.85	–245.3	–31.67	8.1	377-YuV/74	15.5/39.5	–248.3	–32.03	7.9
377-YuV/8	51.1/3.9	–246.6	–31.79	7.7	377-YuV/73	15.0/40.0	–246.9	–31.91	8.4
377-YuV/7	51.05/3.95	–245.7	–31.73	8.1	377-YuV/44	15.0/40.0	–246.6	–32.02	9.6
377- YuV/6	51.01/3.99	–246.2	–31.68	7.2	377-YuV/43	14.8/40.2	–247.1	–31.95	8.5
377- YuV/12	50.9/4.1	–246.5	–31.73	7.3	377-YuV/42	14.6/40.4	–247.2	–31.99	8.7
377-YuV/13	50.8/4.2	–244.1	–32.01	12.0	377-YuV/41	14.4/40.6	–247.8	–32.05	8.6
377-YuV/14a	50.71/4.29	–245.4	–31.83	9.2	377-YuV/51	14.4/40.6	–246.9	–31.96	8.8
377-YuV/14b	50.7/4.3	–246.5	–31.92	8.9	377-YuV/52	14.4/40.6	–246.2	–31.88	8.8
377-YuV/15	50.55/4.45	–249.8	–32.10	7.0	377-YuV/53	14.4/40.6	–246.2	–31.93	9.2
377-YuV/16	50.4/4.6	–249.7	–32.07	6.9	377-YuV/54	14.4/40.6	–246.8	–31.99	9.1
377-YuV/17	50.25/4.75	–252.0	–31.93	3.4	377-YuV/55	14.4/40.6	–246.9	–32.05	9.5
377-YuV/3	50.1/4.9	–257.7	–32.91	5.6	377-YuV/56	14.4/40.6	–246.3	–32.03	9.9
377-YuV/18	50.01/4.99	–250.7	–31.81	3.8	377-YuV/57	14.4/40.6	–246.6	–32.14	10.5
377-YuV/4	50.0/5.0	–247.5	–31.71	6.2	377-YuV/58	14.4/40.6	–246.4	–32.00	9.6
377-YuV/19	49.9/5,1	–250.2	–31.79	4.1	377-YuV/59	14.4/40.6	–244.9	–31.86	10.0
377-YuV/20	49.75/5.25	–252.1	–32.00	3.9	377-YuV/60	14.4/40.6	–238.8	–30.80	7.6
377-YuV/1	49.51/5.49	–256.6	–32.66	4.7	377-YuV/61	14.4/40.6	–248.8	–30.08	7.8
377-YuV/21	49.5/5.5	–251.0	–32.06	5.5	377-YuV/62	14.4/40.6	–249.4	–32.06	7.1
377-YuV/22	49.31/5.69	–252.0	–32.22	5.8	377-YuV/63	14.4/40.6	–250.1	–32.16	7.2
377-YuV/2	49.3/5.7	–255.5	–32.66	5.8	377-YuV/64	14.4/40.6	–250.5	–32.15	6.7
377-YuV/23	49.1/5.9	–252.2	–32.22	5.6	377-YuV/65	14.4/40.6	–249.9	–32.15	7.3
377-YuV/24	48.7/6.3	–251.4	–32.15	5.8	377-YuV/66	14.4/40.6	–249.7	–32.20	7.9
377-YuV/25	48.55/6.45	–255.5	–32.59	5.2	377-YuV/67	14.4/40.6	–248.5	–32.10	8.3
377-YuV/26	48.35/6.65	–257.0	–32.80	5.4	377-YuV/68	14.4/40.6	–246.8	–31.91	8.5
377-YuV/27	48.15/6.85	–257.4	–32.87	5.6	377-YuV/69	14.4/40.6	–246.8	–31.91	8.5
377-YuV/28	48.0/7.0	–257.5	–32.91	5.8	377-YuV/70	14.4/40.6	–247.1	–31.97	8.7
377-YuV/35	47.4/7.6	–256.9	–32.70	4.7	377-YuV/71	14.4/40.6	–244.7	–31.65	8.5
377-YuV/36	46.85/8.15	–260.2	–33.11	4.7	377-YuV/72	14.4/40.6	–243.7	–31.49	8.2
377-YuV/37	46.7/8.30	–259.5	–33.02	4.7	377-YuV/40	14.1/40,9	–248.0	–32.02	8.2
377-YuV/48	20.0/35.0	–235.0	–30.46	8.7	377-YuV/39	14.0/41.0	–247.8	–31.98	8.0

[a] Top of Duvanny Yar section in 1999 at 55 m asl; bottom at 6 m asl. asl = Above sea level; bgs = below ground surface.

Appendices

Appendix S1. Previous ^{14}C Geochronology of the Yedoma (Ice Complex) at Duvanny Yar

^{14}C ages obtained in previous studies of the yedoma at Duvanny Yar (unit 4 of the present study) since 1972 are plotted in Figure 4 and details are given in Tables S1–S4. Age inversions are common in syngenetic permafrost sediments. Some investigators (e.g. Kaplina, 1986) have suggested that the lower 10 m of the cross-section at Duvanny Yar are older than 50,000–40,000 ^{14}C BP, consistent with the age model presented in the present study (Figure 23). One interpretation of such old ages is that they record a considerable admixture of old allochthonous material. Significantly, the base of the yedoma has a dome shape because bluish-grey clay underlies the river level in the marginal parts of the cross-section and crops out above river level only in the central part (unit H1 in Figure 3A). Thus, organic material eroded from the higher central part may have accumulated in inverse order in the lower sections of marginal areas, enriched by old organic material. Thus, only reliable material should be dated, such as layers of autochthonous peat or seed caches within fossil rodent burrows.

Subsequently, an age of 36,900 ^{14}C BP at a height of 8.5 m above sea level (asl) was considered a reliable indicator of the age of some of the lower part of the yedoma, because similar ages have been obtained for the same depth interval: 29,900; 30,100; 31,100; and 35,500 ^{14}C BP (Y. K. Vasil'chuk, 1992, 2006; Gubin, 1999). From the youngest series of ages, the lower 25–30 m of yedoma may date from 40,000–35,000 ^{14}C BP; a high concentration of old organic material is characteristic of this part of the section and leads to irregular results from ^{14}C dating. This interpretation that the lower part of the yedoma dates to 40,000–35,000 ^{14}C BP, however, is distinctly younger than the age model proposed for the lower part of the composite section in the present study (Figure 23).

Pollen spectra of ^{14}C-dated samples have been used to evaluate the amount of allochthonous organic material within the yedoma. Relatively high percentages of *Betula* sect *Nanae* (≤ 19%), the presence of *Pinus pumila, Larix* sp., *Betula* sect *Albae*, *Alnaster* sp. and *Ericaceae* characterise pollen spectra from the lower part of the section at Duvanny Yar. This may be related both to the occurrence of redeposited pollen and spores, and to warmer summer temperatures relative to those relating to the upper part of the section. The regional pollen rain is inferred from pollen spectra obtained from ice-wedge ice, i.e. pollen which entered frost cracks during spring. The key species present within the wide syngenetic ice wedges of the lower part of the yedoma are *P. pumila*, *Betula* sect *Nanae*, *Artemisia* sp., immature herb pollen and *Selaginella sibirica* (Table 2).

The upper part of the yedoma is dated 30,000–13,000 ^{14}C BP, if we consider only the youngest ages for every layer: 13,080 ^{14}C BP from soil at 51 m asl; 19,480 ^{14}C BP from horse bone at 45 m asl; and 28,100 ^{14}C BP from soil at 36 m asl. Older ages at the same levels indicate the presence of allochthonous organic material. The pollen spectra from the upper part of the yedoma are characterised by low percentages of shrub pollen and abundant immature herb pollen together with spores of *S. sibirica*. These pollen and spores are often found in the yedoma of northern Yakutia and have been thought to record environmental conditions of yedoma accumulation (and possibly inundation) when immature herb pollen was mixed on floodplains during rapid accumulation of the sediment. The same process also caused redeposition of allochthonous organic material. Pollen spectra from the narrow ice wedges in the upper part of the yedoma are dominated by *Poaceae*, *Artemisia* sp. and *Betula* sect. *Nanae*. In summary, the pollen data suggest that redeposition of organic material was more probable during accumulation of the lower part of the yedoma than during the upper part.

The upper part of the yedoma has been previously considered to have accumulated faster than the lower part (Table S2). This is supported by the external appearance of the large syngenetic ice wedges. The upper ice wedges are narrow—attributed to rapid accumulation of their host sediments and vertical ice-wedge growth—whereas the lower ice wedges are considerably wider, attributed to slower sediment accumulation and growth (cf. Kaplina *et al.,* 1978). Possibly, subaerial stages dominated during deposition of the lower part, which is evident from the occurrence of horizontal peat layers in the lower part; for example, one such layer of pure peat at 8.5 m asl has provided an age of 36,900 ^{14}C BP. The ice in the upper ice wedges contains an admixture of loam and sandy loam (i.e., composite ice-soil wedges), whereas the ice of the lower stage is pure. Results from the present study (Table 7), however, suggest that rates of yedoma accumulation varied substantially within the upper 13 m of unit 4.

Comparison of ^{14}C ages from a bulk sample of yedoma with AMS ages from different organic fractions supports our assumption that the youngest ^{14}C ages are more reliable indicators of the true depositional age of the sediment than are the older ages. The hot alkaline extract of bulk sample 316-YuV/9, from 14.0 m asl, provided an age of 44,200±1100 ^{14}C BP (GIN-4003) (Table S3). The sample was then separated into three parts: (1) seed fragments, (2) thin white twigs without crust (about 0.5–1 mm), and (3) herb remains and detritus (≤ 0.5 mm). AMS ages obtained from fractions (1) and (2) indicate the presence of old allochthonous organic material in this sediment (Table S3). The age from the herb remains is more than 5,000 ^{14}C younger than the age of the bulk sample; even the youngest age is older than time of sedimentation and is thought to indicate redeposition of dated material. Possibly, the sediments at 14.0 m asl are younger. The age of the bulk sample is similar to the oldest age, which was obtained from the seed fragments. The sample 316-YuV/5 from the lower part of this cross-section (9.8 m asl) was dated in by hot alkaline extract to 44,600±1200 ^{14}C BP (GIN-4000). Insect fragments from this sample were AMS dated to 34,900±800 ^{14}C BP (SNU01-076). These data fit well into the range of the youngest ages (Table S2). In conclusion, the youngest ages are considered the most reliable indicators of depositional age in syngenetic permafrost sediments.

A relatively young age (approximately 30,000 ^{14}C BP or younger) for the beginning of yedoma accumulation has been supported by ^{14}C ages from organic material within ice-wedge ice (Table S4, Figure 3B). The ages of microinclusions from ice wedges have confirmed that the youngest ice wedges occur in the middle stream fragment of the exposure. This suggests that the upper part of Section 3 on Figure 3B accumulated towards the end of the period of yedoma formation.

Y. K. Vasil'chuk (2006) has summarised the results of radiocarbon and stable-isotope studies of Duvanny Yar during the previous 50 years and considered the vertical and lateral variations in structure, sedimentary cycles and age of the yedoma. Macro- and mesocycles in sedimentation are inferred during the long and complex history of yedoma accumulation; they differ in the central and peripheral parts of the exposure. According to Y. K. Vasil'chuk, the initial stage of freezing and the formation of ice-rich sediments took place under a broad and shallow lake on a floodplain, with frost heave raising the central part of the yedoma area. Mesocycle lake bog and fluvial sediment accumulation occurred for several thousand years between 37,000 ^{14}C BP (maximum 41,000 ^{14}C BP) and 31,000 ^{14}C BP, and led to the formation of the yedoma in the lower, central part of the exposure. During this first phase of yedoma accumulation, subaqueous conditions were repeatedly interrupted by long periods of subaerial bog-floodplain sedimentation characterised by active growth of ice wedges. Interruptions of the subaqueous regime, however, were local in extent: peaty horizons accumulated in some places, while sandy loam almost free in organic material accumulated in others. Therefore, the peaty horizons occur as large but discontinuous lenses. By the end of macrocycle I, frost heave of a few metres had occurred in the central part of the yedoma exposure and subsequent drainage had taken place between about 31,000 and 24,000 ^{14}C BP. As a result, ice-wedge growth in the first macrocycle stopped in the greater part of the Duvanny Yar yedoma.

Sedimentation varied spatially during the final stage of yedoma accumulation. In the highest, central part—where the yedoma is thicker than 50 m and the yedoma surface is more than 50 m asl—sedimentation probably ended earlier than in other parts, because the centre was above the water level. Therefore, older yedoma horizons had formed on the subsurface of the central section. In the upper section of the central part of the yedoma body, the younger yedoma of macrocycle II actively formed, probably due to temporary resumption of soil and peat accumulation. During macrocycle II, the accumulation of yedoma took place in the central part of the site at the same time as peripheral parts were actively eroded. At about 24,000–23,000 ^{14}C BP, the lacustrine basin with narrow ice wedges of macrocycle II in the central part shifted-off centre or formed a semicircle and abraded the highest central dome, probably due to an additional uplift of the area. The growth of ice wedges may have continued epigenetically, as suggested by the ice-wedge sample dated at 19,000 ^{14}C BP. As a result of the partial re-working of the central dome, an alas-type lacustrine basin produced a terrace-shaped bench on the slope, resulting in the formation of a terrace-like yedoma of younger sedimentary material; all the ice samples from this site yielded ages of less than 25,000 ^{14}C BP, and the youngest ice wedges (16,000–14,000 ^{14}C BP or less) are assigned to macrocycle III.

Appendix S2. Palaeotemperature Significance of Stable-Isotope Records from Syngenetic Ice Wedges

Stable-isotope values from syngenetic ice wedges at Duvanny Yar allow precise reconstruction of winter air palaeotemperatures for the last 30,000–40,000 ^{14}C yrs. The reconstructions are based on the strong empirical relationship between the δ^{18}O values in modern syngenetic ice wedges ($\delta^{18}O_{iw}$) and mean January air temperatures ($t_{mean\ January}$), reflecting the atmospheric origin of water (snow), which constitutes the main source for the ice wedges when the snow melts in early spring. Hence, δ^{18}O values from ice-wedge ice provide an indicator of winter air temperature at the time of snow formation. Palaeotemperature estimates are time-averaged bulk samples of ice-wedge ice formed during numerous episodes of crack filling; thus, extreme winter temperatures are averaged out.

These relationships are expressed in the following simplified regression equation (Y. K. Vasil'chuk, 1992):

$$t_{mean\ January} = 1.5\ \delta^{18}O_{iw}\ (\pm 3^{o}C) \qquad (1)$$

The correlation coefficients are 0.95–1.0 in most regions of the Eurasian permafrost zone. The equation shows that more negative δ^{18}O values correspond with severe winters, and the more positive values with warmer ones (Y. K. Vasil'chuk, 1992, 2006).

Ice wedges at Duvanny Yar were sampled in autumn 1985—at the time of maximum opening of the yedoma exposure—from 3 sections (316-YuV, 319-YuV, 320-YuV) and in summer 1999 from 2 sections (377-YuV) (Figure S1). The sampled sections are shown schematically in Figure 3B and the data are plotted in Figure S2. The δ^{18}O values in the samples collected in 1985 were analysed in the Geology Institute of Estonian Academy of Sciences, Tallinn; and δ^{18}O and δD values in the samples collected in 1999 were obtained in the Arsenal, Vienna. Sampling was performed both vertically and horizontally from large ice wedges, in order to exclude the gaps in the isotope record of the wedges. The similar ranges of isotope variations in both vertical and horizontal sampling suggest the absence of omissions in the isotope record. As a result, the vertical sample data were used to evaluate the chronological sequence, because the syngenetic ice wedges become younger from bottom to top.

The δ^{18}O values vary from −29.8 to −33.11‰, and δD values from −235.0 to −260.2‰. For comparison, δ^{18}O values from modern ice wedges of the Kolyma River floodplain vary between –26.1 and –23.0‰. The ice wedges exposed at 15–25 m asl have similar isotope values and trends for both the 1985 and 1999 samples (Figure S2; Tables S5 and S6), even though the layers in the yedoma are not horizontal. In addition, the δ^{18}O values show a cyclical sawtooth pattern (Figure S2), especially in the isotope plot of samples from 1985. There are three cycles of isotopically more positive ice (δ^{18}O values > −30.5‰) which are separated by two cycles of isotopically more negative ice (δ^{18}O values < −32.0‰).

Detailed horizontal sampling was performed over each 10-cm increment from a large ice wedge at +14.4 m asl in 1999 (Figure S2). The essential coincidence of δ^{18}O and δD plots points to the atmospheric origin of ice-wedge water. However, the subvertical marginal zones of ice wedges (about 10–20 cm thick) are isotopically heaver (δ^{18}O by 1–1.2‰, and δD by 6‰) than the main part of the wedges and so cannot be used for palaeotemperature reconstruction. It has been suggested that this ice formed in the initial stage, when river or lake-water entered the cracks. Slow isotopic exchange (by diffusion with host sediments) is an additional or alternative explanation for the isotopically heavier marginal ice.

Mean January air temperatures during accumulation of yedoma at Duvanny Yar varied from −45 to −49.5 ^{o}C. In the Bison Section on the lower Kolyma River, 15 km downstream of Duvanny Yar (Figure 2A), almost constant values of δ^{18}O and δD obtained from syngenetic wedge ice ^{14}C dated to 33,000–26,000 ^{14}C BP indicate very stable winter palaeoclimate conditions during this interval (Y. K. Vasil'chuk *et al*., 2001b, 2003). Average winter air temperature variations did not exceed 1°C (from –32 to –33°C) and average January air temperature variations did not exceed 2°C (from –48 to –50°C), both much colder than modern values of –24 and –35°C, respectively. δ^{18}O values of syngenetic wedge ice dated by AMS measurements of micro-organic inclusions and pollen concentrates to between 32,600 and 11,400 ^{14}C BP—from Duvanny Yar, Bison and Plakhinskii Yar in the lower Kolyma River region (Figure 2A)—were significantly lower than Holocene values, and have been correlated with Dansgaard-Oeschger events inferred from the Greenland ice cores (Y. K. Vasil'chuk and A. C. Vasil'chuk, 2008).

Appendix S3. Pollen Spectra from Ice Wedges at Duvanny Yar

Pollen spectra in ice wedges contain pollen and spores accumulated in the snow cover during winter and spring. The pollen rain consists of pollen blown from the southern areas, because plants are blooming and producing pollen earlier than those in the areas where ice wedges tend to form. Additionally, strong winter winds may deflate pollen and spores from exposed ground closer to the ice wedges and mix them into the snow. A pretreatment procedure for pollen analyses and AMS ^{14}C dating of ice samples from Late Pleistocene syngenetic ice wedges is given by A. C. Vasil'chuk *et al.* (2005) and dating of pollen concentrate and particulate organic matter in such ice is reviewed by Lacelle and Y. K. Vasil'chuk (2013). Pollen and spore concentrates from ice-wedge ice at Duvanny Yar were dated in the AMS facility of Seoul National University. Pollen identifications were carried out before and after the treatment had been completed, in order to identify what pollen species were preserved after pretreatment and dated.

Pollen spectra from ice-wedge ice collected in the 1985 and 1999 sampling programmes by A. C. Vasil'chuk and Y. K. Vasil'chuk at Duvanny Yar are summarised in Figures S3 and S4. Tree pollen tends to be more common in the lower parts of the ice wedges, whereas Poaceae and *Artemisia* sp. are particularly abundant in their upper parts (Figure S3). This overall trend is broadly consistent with the pollen data from the surrounding yedoma silt, which records in the upper part of the yedoma a trend towards treeless tundra-steppe with abundant grasses and *Artemisia* sp. (Table 2; Kaplina *et al.,* 1978; Sher *et al.,* 1979).

A key feature of the Duvanny Yar pollen data is the stable ratio between local components of the vegetation, which suggests that sediment accumulated during stable local environmental conditions (A. C. Vasil'chuk, 2007). The local vegetation contains various herbs and *Selaginella sibirica*. High percentages of *Varia* and *Poaceae* correspond to minimal salt concentrations, whereas a peak in *S. sibirica* corresponds to maximum salt concentration. *Larix* pollen suggests that isolated larch trees were present. Three small peaks of *Artemisia* (4.5–5.1%) indicate short-term dry periods.

Changes of vegetation inferred at the same time intervals at a number of sites in the Kolyma Lowland (A. C. Vasil'chuk, 2007; Y. K. Vasil'chuk and A. C. Vasil'chuk, 2008) may correspond with Heinrich events in the North Atlantic Ocean (Bond *et al.,* 1997; Veiga-Pires and Hillaire-Marcel, 1999; Vidal *et al.,* 1999; Ivy-Ochs *et al.,* 2006; Parnell *et al.,* 2007; Sepulchre *et al.,* 2007). The expression of every event is specific. Sediment at 15–19 m depth is assumed to have accumulated during 29,000–27,000 ^{14}C BP and correlated with Heinrich Event (H) 3. The succeeding increase of *Poaceae* may correlate with a warm phase and the subsequent maximum of *Artemisia* may correlate with H2 (23,000–21,000 ^{14}C BP). The upper part of the record shows a typical distribution of the components for H1 (16,500–14,000 ^{14}C BP; A. C. Vasil'chuk, 2007): from bottom to the top are observed opposite fluctuations of *Poaceae* and *Artemisia* pollen and a subsequent local maximum of *Betula* sect. *Nanae*.

Pollen spectra from ice wedges demonstrate regional peculiarities of two rhythms of vegetation cover changes (Figure S3). The lower one (11.6–21 m depth) is similar to the lower rhythm of ice-wedge spectra from Zelyony Mys (Figure 2A). Maximum percentages of spores correspond to a *Poaceae* peak, which is replaced by *Artemisia* and then by a peak in *Varia*. We compare this rhythm to H2 (23,000–21,000 ^{14}C BP). The structure of the upper rhythm (11.6–5.5 m depth) is similar to variations of the main components observed in pollen spectra from ice wedges of Plakhinski Yar (Figure 2A). The fluctuations of *Poaceae* and *Artemisia* pollen are opposite. The *Betula* sect. *Nanae* peak follows *Artemisia*. This rhythm corresponds to H1 (16,500–14,000 ^{14}C BP).

H1 may be separated into three phases on the basis of pollen plots of the syngenetic sediments and ice wedges. The first phase corresponds to relatively high temperatures and normal humidity, nival meadows and Pleistocene mesic tundra with a mosaic of shrubs and trees (*Betula* and *Larix*). The second phase corresponds to low temperatures during the growing season, a very short vegetation season and low humidity, and maximum distribution of nival meadow vegetation (*Varia* and *S. sibirica* or *Bryales*). The regional pollen rain is characterised by a prevalence of *Artemisia*. The third phase corresponds to relatively high temperatures and increasing humidity. *Poaceae* and *Varia* dominate, and *Pinus pumila* occurs in the regional pollen rain.

H2 is expressed by a changing combination of peaks of *Poaceae* and *S. sibirica*, by maximum amounts of immature *Varia* pollen, and then by appearance of *P. sibirica* pollen. This rhythm in the Lower Kolyma plain was asymmetrical. The warm phase before the thermal minimum was relatively dry and long compared to the thermal minimum itself. Differences between the local and regional pollen rain are inferred. The maximum distribution of nival-meadow vegetation coincided with the appearance of *Pinus* pollen.

H3 is characterised by consecutive change of local peaks of *Betula* sect. *Nanae*, *Poaceae* and *Artemisia* and disappearance of *P. pumila*. H4 (35,000 ^{14}C BP or more) is characterised by absolute maximum of *S. sibirica*, followed by a sharp decrease of total concentration of pollen and then twin a peak of *Poaceae* and *Artemisia* and *Betula* sect. *Nanae* percentages growth.

These sharp oscillations of pollen and spores were caused by global changes and are recorded in other pollen plots of polygonal yedoma units of northern Eurasia.

Appendix S4. Pollen Spectra of the Modern Surface of the Lower Kolyma Region and of Units 1, 4 and 5 at Duvanny Yar

Pollen spectra collected by Andrei Sher in the lower Kolyma region are shown in Figure S5. The eight samples derive from *Larix* forest, forest-tundra and tundra. The samples are similar in composition to the Holocene samples collected in the 2009 study. Figure S6 compares the modern pollen samples from the lower Kolyma region with pollen samples from different pollen zones and stratigraphic units at Duvanny Yar (Holocene samples in zone A from the near-surface silt of unit 5, LGM samples from zone B in yedoma silt of unit 4, pre-LGM and post-LIG samples from zones C and D of unit 4 [Figure 26], and MIS 6 samples from massive silt of unit 1 [Figure 25]) via an ordination (detrended correspondence analysis, DCA, implemented with PC-ORD, McCune and Mefford, 2011). Rare species were downweighted. After examining the ordination with all species and samples, and assessing outliers, Poaceae and two samples, DY01, the LIG sample (90% pine), and sample DY110 (60% Caryophyllaceae) were excluded. The first and second eigenvalues were 0.37 and 0.19, respectively; removal of outliers reduced the first two axis lengths both to 2.4, which is not ideal, but there remains a clear gradient on axis 1 of modern and Holocene samples (to the right, characterised by taxa such as *Betula, Alnus*, Ericales, *Salix, Valeriana*, *Sphagnum, Larix* and Cyperaceae) to samples characterized by a range of forbs (e.g. Asteraceae, Caryophyllaceae, Primulaceae) and *Selaginalla rupestris*. *Pinus* lies in the middle of the gradient, reflecting its appearance in many samples, including those dating to the LGM and MIS 3. LGM samples are not distinguishable from MIS 3 and MIS 6 samples.

Appendix S5. Palaeosol Correlations between the 2009 Study and Previous Studies at Duvanny Yar and Stanchikovsky Yar

The five palaeosols identified in yedoma silt (unit 4; Figure 5) in the present study at Duvanny Yar are thought to correlate with those identified previously by Zanina *et al.* (2011, fig. 4). The potential correlations are, in order of increasing depth beneath the yedoma surface:

- Palaeosol 5 = Late Karginsky third-stage buried soil 4: 28,000 ^{14}C BP
- Palaeosol 4 = Late Karginsky second-stage buried soil 3: 33,000–31,000 ^{14}C BP
- Palaeosol 3 = Late Karginsky first-stage buried soil 2: 38,000–35,000 ^{14}C BP
- Palaeosol 2 = Early Karginsky buried soil 1: 44,000–42,000 ^{14}C BP

Each palaeosol is described below in general terms, mainly from investigation of the 6E yedoma remnant (Figure 3A) during the 2002 field season, incorporating observations collected by S. V. Gubin since 1978 (Gubin, 1984, 1994, 1998, 2002). The ages given below, however, are all at least a few thousand ^{14}C years younger than those in section CY and incorporated into our new age model (Figures 5 and 23), and so they should be regarded as minimum ages.

Palaeosol 2 = Early Karginsky buried soil 1: 44,000–42,000 ^{14}C BP

Autochthonous peat about 12 m arl and forming a 1.5–2.0 m thick layer overlies lacustrine-alas talik deposits in the downstream part of the Duvanny Yar exposure (5.5–7.5 km on Figure 3A). ^{14}C dating of the peat indicates an age of 44,000–42,000 ^{14}C BP, the warmest period of MIS 3 (Kaplina, 2011; Zanina *et al.,* 2011). The peat contains the remains of sedges, mosses, shrubs and large trees (mainly *Larix sp.*). Further downstream (8–9 km on Figure 3A), the peat and lacustrine-alas deposits grade into cryopedolith. In the upstream part of Duvanny Yar (0–2 km on Figure 3A), the peat can be observed very locally at a height of 6–7 m arl, where it is thinner, contains rounded branches of shrubs and willows, and is overlain by cryopedolith silty loam. In the downstream part of the Duvanny Yar exposure, massive peat underlies yellowish sand with thin cross-bedded layers. Peat also contains silty and clayey layers with abundant *in situ* roots. The peat formed during the first cycle of Karginsky stage epigenic pedogenesis.

Palaeosol 3 = Late Karginsky first-stage buried soil 2: 38,000–35,000 ^{14}C BP

A peaty soil profile with buried sedge tussocks overlies yellowish sand. In 1991, this soil profile was about 20 m arl (Figure S7A). During the following 20 years of river bank retreat, we have observed the spatial structure of the buried soil extending by more than 80 m into the bank. Peat is mainly present with weakly decomposed plant residues, waterlain fragments of moss and sedge peat with silty thin-bedded lenses, rounded branches of trees and shrubs, and rare water-stable soil aggregates. The peat also contains thin (<20 cm thick) layers of puddled sedge detritus with abundant excrement of small rodents. Radiocarbon ages of the samples from this layer vary from 38,000–35,000 ^{14}C BP (moss or sedge peat) to 48,000–40,000 ^{14}C BP (buried rounded tree remnants). In recent years, this complicated buried soil layer has cropped out as a layer of allochthonous peat 2.5–3.0 m thick.

In the downstream part of the Duvanny Yar exposure (5–9 km on Figure 3A) the allochthonous peat grades into the layer of grayish silty sand with abundant tree branches and weakly decomposed sedges previously interpreted as river channel facies. Peaty soil with buried 30–40 cm thick sedge tussocks is often observed in the upper part of the sand layer. The allochthonous peat and buried peaty soil are both distinguished as Late Karginskian first-stage buried soil 2.

Palaeosol 4 = Late Karginsky second-stage buried soil 3: *33,000–31,000 ^{14}C BP*

A gleyic peaty buried soil at about 27 m arl occurs within massive grayish cryopedolith (Figure S7B). It is well-expressed all along the exposure and formed in less hydromorphic conditions than palaeosol 3, but it also has features attributed partially to waterlain deposition of mineral material (thin-bedded silt and sand with possible evidence of water sorting). It has gleyic features in the middle and lowermost part of the mineral profile. The uppermost peaty horizon is about 30–40 cm thick, enriched with silt and contains remains of sedge tussocks. Profile organisation, horizon properties and morphology are similar all along the exposure. The radiocarbon age of peat samples from the upper soil horizon is about 33,000–31,000 ^{14}C BP, and the soil is distinguished as Late Karginskian second-stage buried soil 3.

Palaeosol 5 = Late Karginsky third-stage buried soil 4: *28,000 ^{14}C BP*

The youngest buried soil is located in the grayish silty loams of cryopedolith at 30–32 m arl and clearly expressed in the downstream yedoma remnants (5–9 km on Figure 3A). The soil profile is weakly differentiated and mineral horizons are slightly gleyic, with small amounts of weakly decomposed plant detritus. The uppermost brownish peaty horizon contains weakly decomposed sedge and herb remains with some moss detritus. Significant features of this soil are silt enrichment in the organic horizon, and the small amount of segregated ice in mineral horizons and in the palaeotransient layer. The soil is thought to have formed in dry climate conditions and to be intermediate in its development between gleyic peaty soils and cryosynlithogenic soils (cryopedoliths). In some parts of the Duvanny Yar exposure the uppermost horizons of this buried soil are dark brown and contain well-decomposed plant detritus (according to micromorphological and loss-on-ignition data). With a ^{14}C age of plant samples from the upper soil horizon of about 28,000 ^{14}C BP, the soil is distinguished as Late Karginskian third-stage buried soil 4.

Root-enriched palaeosol

S. V. Gubin and O. G. Zanina have observed a root-enriched palaeosol—correlated here with Palaeosol 1 in Figure 5—at a depth of 6–7 m below thick autochthonous peat within yedoma remnants 6E and 7E. Full description and sampling of this soil, however, were handicapped because of active thaw slumping. The profile thickness of the soil is about 1.5 m. The uppermost horizon is peaty with distal parts of roots (70–80 per m^2), and the mineral parts of the profile are slightly gleyic. The soil is underlain by grayish sandy banded cryopedolith.

Palaeosols at Stanchikovsky Yar

Similar palaeosols within yedoma deposits have been observed at Stanchikovsky Yar, near the settlement of Anyuysk, 100 km east of Duvanny Yar (Figure 2A). The Stanchikovsky Yar exposure, located beside the Malyy Anyuy River, is about 250 m long and 50 m high (Figure S8). Since the late 1980s three buried palaeosols have been studied in four thaw slumps along the exposure. The lowermost part of the exposure is nearly always covered with thick cliff debris.

The lowermost 12 m of deposits comprise monotonous grayish sandy silts (interpreted as lacustrine) containg rare plant residues, including shrub branches, sedge-grass detritus and peat fragments. They are overlain by 1.5–2.5 m thick dark-brown sandy silt enriched with peat and with well-expressed features of gleyization, which commonly grades into icy allochthonous peat enriched with sand and fragments of trees, shrubs and grass. This thick layer of sandy peat is similar to the Early Karginsky buried soil 1 (Palaeosol 2) at Duvanny Yar. Its ^{14}C age varies between 47,000 and 37,000 ^{14}C BP.

The first buried palaeosol at Stanchikovsky Yar is 24 m arl. It formed on brownish cryopedolith and has gleyic features in the middle and lowermost parts of the profile. Rarely, the uppermost horizon has features of organic matter humification. The upper parts of the soil profile may contain lemming burrows and tunnels. The soil moisture regime is likely to have varied significantly across the land surface. The ^{14}C age of this palaeosol is about 40,000–37,000 ^{14}C BP; a few samples have provided ages of 47,000–42,000^{14}C BP, which is close to the limit of ^{14}C dating. The soil is correlated with the Late Karginsky first-stage buried soil 2 (Palaeosol 3) at Duvanny Yar.

The second buried gleyic palaeosol is about 32 m arl. Its profile structure is similar to the palaeosol just described, but it is extremely ice-rich (>150% of total volume) and its thickness in the frozen wall may reach 3 m. The uppermost peat horizon is enriched with silt and often contains buried sedge tussocks. Spore-pollen data from the uppermost horizons are problematic to interpret because they show the dominance of shrubs, grasses and trees despite hydromorphic features in mineral horizons of the soil profile. The ^{14}C age of this palaeosol is about 34,000 ^{14}C BP, which enables it to be correlated with the Late Karginsky second-stage buried soil 3 (Palaeosol 4) at Duvanny Yar.

The third palaeosol at Stanchikovsky Yar is 40 m arl and formed on gray ice-rich cryopedolith. This soil horizon is transitional between peat and coarse humus and contains highly mineralised plant detritus. The ^{14}C age of peat material is about 28,000 ^{14}C BP, which strongly favours correlation of this palaeosol with the Late Karginsky third-stage buried soil 4 (Palaeosol 5) at Duvanny Yar.

Conclusion

In conclusion, the yedoma deposits of the Kolyma Lowland contain four main buried epigenic soil profiles that are thought to have formed during MIS 3. We suggest that there was no significant deposition of mineral material during the soil-forming periods and that pedogenic processes took place in the stable volume of the mineral material, forming soil horizons (Gubin, 1994). The majority of buried soil profiles are underlain by an ice-rich transition zone similar to that associated with Holocene soils (Shur, 1988a, 1988b; Gubin and Lupachev, 2008). Due to the significant volume of ground ice in buried soil profiles, the apparent thickness of soil horizons can exceed their original (unfrozen) thickness by two to three times. Such exaggerated thicknesses of soil horizons should be considered while conducting soil studies.

Appendix S6. References

Bond G, Showers W, Cheseby M, Almasi P, deMenocal P, Priore P, Cullen H, Hajdas I, Bonani G. 1997. A pervasive millennial-scale cycle in North Atlantic Holocene and glacial climates. *Science* **278**: 1257–1266. DOI: 10.1126/science.278.5341.1257.

Gubin SV. 1998. Soil formation during the Sartan Cryochron in the Western sector of Beringia. *Eurasian Soil Science Meeting, Program and Abstracts* **31**: 547–550.

Ivy-Ochs S, Kerschner H, Kubik PW, Schluchter C. 2006. Glacier response in the European Alps to Heinrich Event 1 cooling: the Gschnitz stadial. *Journal of Quaternary Science* **21**: 115–130. DOI: 10.1002/jqs.955.

Kaplina TN. 2011. Ancient alas complexes of Northern Yakutia (Part 1). *Earth Cryosphere* **15**: 3–13. (in Russian).

Lacelle D, Vasil'chuk YK. 2013. Recent progress (2007–2012) in permafrost isotope geochemistry. *Permafrost and Periglacial Processes* **24**: 138–145. DOI: 10.1002/ppp.1768.

Parnell J, Bowden S, Andrews JT, Taylor C. 2007. Biomarker determination as a provenance tool for detrital carbonate events (Heinrich events?): Fingerprinting Quaternary glacial sources into Baffin Bay. *Earth and Planetary Science Letters* **257**: 71–82. DOI:10.1016/j.epsl.2007.02.021.

Sepulchre P, Ramstein G, Kageyama M, Vanhaeren M, Krinner G, Sanchez-Goni M-F, d'Errico F. 2007. H4 abrupt event and late Neanderthal presence in Iberia. *Earth and Planetary Science Letters* **258**: 283–292. DOI:10.1016/j.epsl.2007.03.041.

Vasil'chuk A. 2007. *Palynology and Chronology of Polygonal Ice Wedge Complexes in Russian Permafrost* Vasil'chuk Yu. (ed.). Moscow University Press: Moscow.

Vasil'chuk A, Kim J-C, Vasil'chuk YK. 2005. AMS ^{14}C dating of pollen concentrate from Late Pleistocene ice wedges from the Bison and Seyaha sites in Siberia. *Radiocarbon* **47**: 243–256.

Vasil'chuk YK, Vasil'chuk AC. 2008. Dansgaard-Oeschger events on Isotope Plots of Siberian Ice Wedges. In *Proceedings of the Ninth International Conference on Permafrost, June 29–July 3, 2008*, Kane DL, Hinkel KM (eds). Institute of Northern Engineering, University of Alaska Fairbanks: Fairbanks, AK; Vol. 2, 1809–1813.

Vasil'chuk YK, Vaikmae RA, Punning J-MK, Lebman MO. 1988. Oxygen-isotope distribution, palynology and hydrochemistry wedge ice in organic-mineral complex of Duvanny Yar type section. *Transactions (Doklady) of the USSR Academy of Sciences, Earth Science Sections* **292**(N5): 69–72.

Vasil'chuk YK, Kim JC, Vasil'chuk AC. 2004. AMS ^{14}C dating and stable isotope plots of Late Pleistocene ice-wedge ice. *Nuclear Instruments and Methods in Physics Research. Section B: Beam Interactions with Materials and Atoms* **223–224**; 650–654. DOI: 10.1016/j.nimb.2004.04.120.

Veiga-Pires CC, Hillaire-Marcel C. 1999. U and Th isotope constraints on the duration of Heinrich events H0–H4 in the southeastern Labrador Sea. *Paleoceanography* **14**: 187–199. DOI: 10.1029/1998PA900003.

Vidal L, Schneider RR, Marchal O, Bickert T, Stocker TF, Wefer G. 1999. Link between the North and South Atlantic during the Heinrich events of the glacial period. *Climate Dynamics* **15**: 909–915. DOI: 10.1007/s003820050321.